

Supplementary Materials for

Bimetal oxides-derived flower-like heterogeneous Co/MnO@C composites with synergistic magnetic-dielectric attenuation for electromagnetic wave absorption

Dongmei Xu^a, Nannan Wu^b, Kai Le^a, Fenglong Wang^b, Zhou Wang^b, Lili Wu^b, Wei Liu^{*a}, Ancheng Ouyang^a, and Jiurong Liu^{*b}

^a State Key Laboratory of Crystal Materials, Institute of Crystal Materials, Shandong University, Shandong, 250100, China

^b School of Materials Science and Engineering, Shandong University, Jinan, Shandong, 250061, China

*Corresponding author.

E-mail addresses: weiliu@sdu.edu.cn

E-mail addresses: jrliu@sdu.edu.cn

Preparation of Co/MnO@C composites.

The 3D flower-like Co/Mn precursors were prepared through a solvothermal process previously reported.¹ Typically, 2.67 mmol $\text{Co}(\text{CH}_3\text{COO})_2 \cdot 4\text{H}_2\text{O}$, 1.33 mmol $\text{Mn}(\text{CH}_3\text{COO})_2 \cdot 4\text{H}_2\text{O}$, and 0.8 g polyvinyl pyrrolidone (PVP, K30) were dissolved in 80 mL ethylene glycol (EG). The solution reacted at 200 °C for 24 h in a Teflon-lined stainless steel autoclave. After centrifugation and repeated washing, the precursors were dried at 60 °C for 12 h. Afterwards, the MnCo_2O_4 microspheres were obtained by calcinating the precursors in air at 400 °C for 1 h. In order to get the 3D flower-like Co/MnO@C composites, 0.88 g MnCo_2O_4 powder was mixed with 0.5 mL pyrrole in a stainless steel autoclave and reacted at 570 °C for 5 h. The sample with an initial addition ratio of cobalt salt and manganese salt equaling 1:2 was also prepared in the same method. The obtained samples with different element ratio were denoted as MC2@C and CM2@C, respectively. The precursor of Co@C and pure Co was prepared through the same method without the addition of manganese salt. The reduction condition of Co@C kept consistent with Co/MnO@C composite. The pure Co particles were prepared by the hydrogen reduction at 350 °C for 1.5 h.

Preparation of MnO@C composites.

The MnO@C composites with the similar size and morphology were also prepared as the control sample.² 1.5 g PVP (K30), 3 mmol $\text{Mn}(\text{Ac})_2 \cdot 4\text{H}_2\text{O}$ and 3 mmol urea were firstly dissolved in 60 mL diethylene glycol (DEG) under magnetic stirring. The mixture solution was then transferred into a 100 mL Teflon-lined stainless steel autoclave and reacted at 200 °C for 24 h in an oven. After the reaction, the brown

precipitate was centrifuged and washed with ethanol. And then the product was dried in an oven at 60 °C for 12h. After annealing at 400 °C for 1 h in air, the Mn₂O₃ microspheres were obtained. To obtain the MnO@C microspheres, 0.88 g Mn₂O₃ power was mixed with 0.5 mL pyrrole in a stainless steel autoclave and reacted at 570 °C for 5 h.

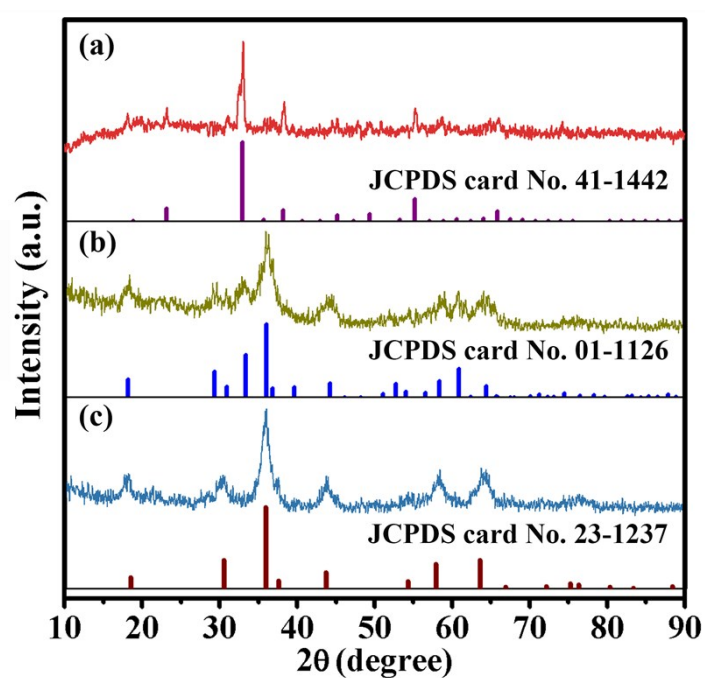


Fig. S1 XRD patterns of Mn₂O₃ (a), CoMn₂O₄ (b) and MnCo₂O₄ (c).

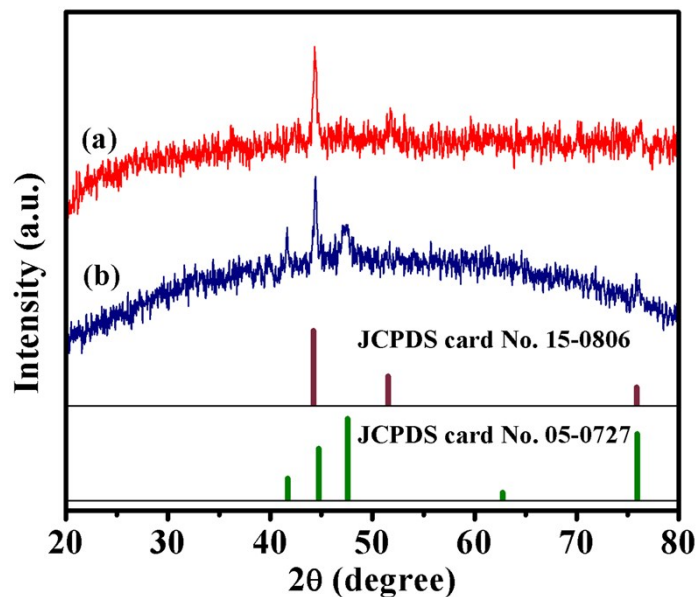


Fig. S2 XRD patterns of Co@C composites (a) and pure Co (b).

The XRD pattern of Co@C (**Fig. S2a**) indicated that the precursor was completely reduced to the face-centered cubic Co (JCPDS card No. 15-0806). While under the hydrogen reduction, both face-centered cubic Co (JCPDS card No. 15-0806) and hexagonal close-packed Co (JCPDS card No. 05-0727) were produced simultaneously.

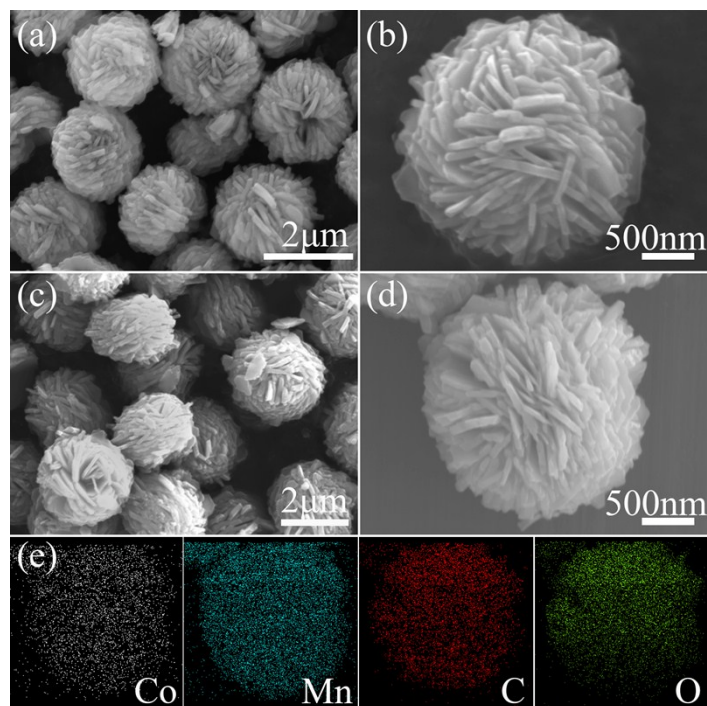


Fig. S3 SEM images of CM2@C precursors (a, b), CM2@C (c, d) and elemental

mapping of CM2@C (e).

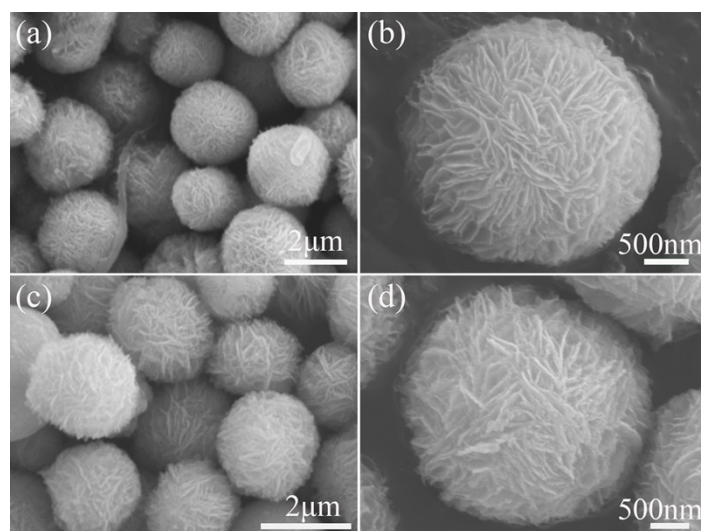


Fig. S4 SEM images of MnO@C precursor (a, b) and MnO@C (c, d).

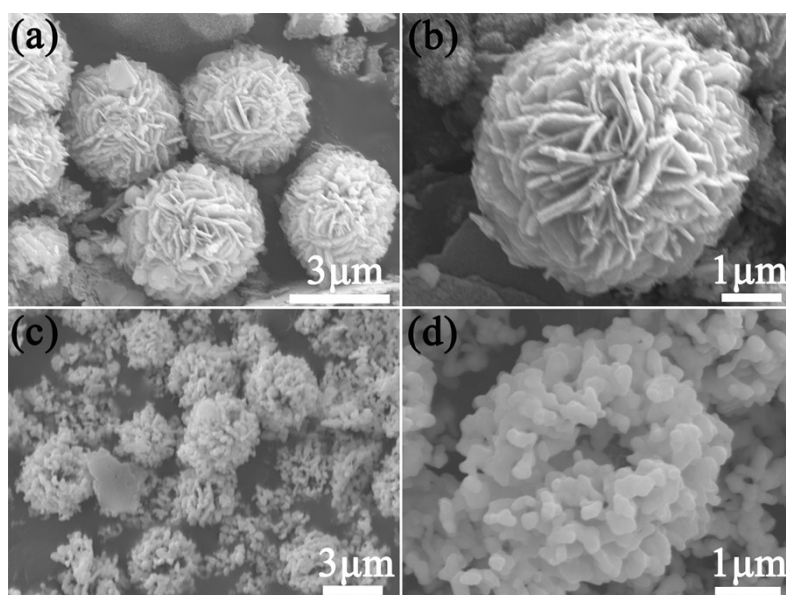


Fig. S5 SEM images of Co@C composites (a, b) and pure Co (c, d).

Table S1. The conductivity of MnO@C, CM2@C and MC2@C composites.

Sample	MnO@C	CM2@C	MC2@C
Conductivity (S/cm)	2.76×10^{-6}	1.76×10^{-5}	5.73×10^{-5}

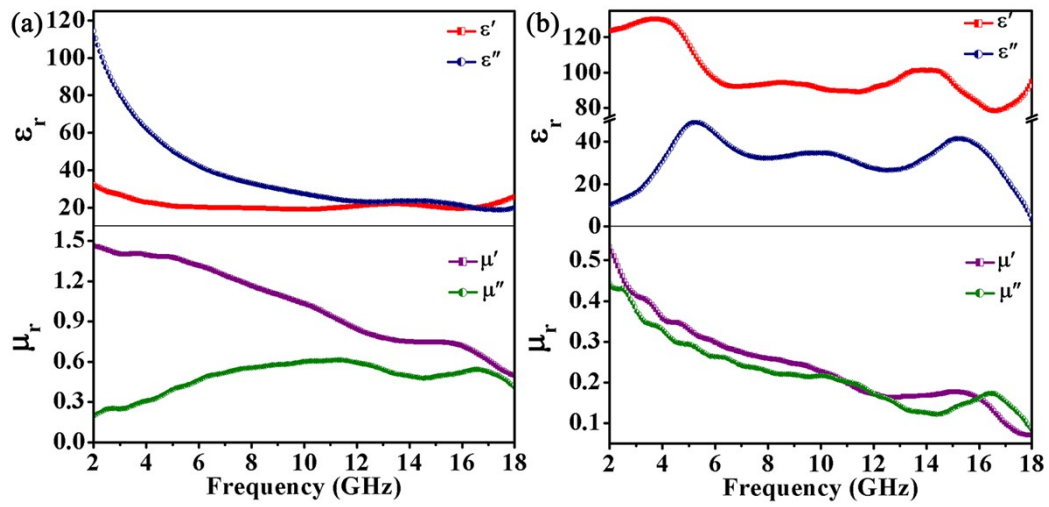


Fig. S6 The relative complex permittivity and permeability of Co@C (a) and Co (b) specimens.

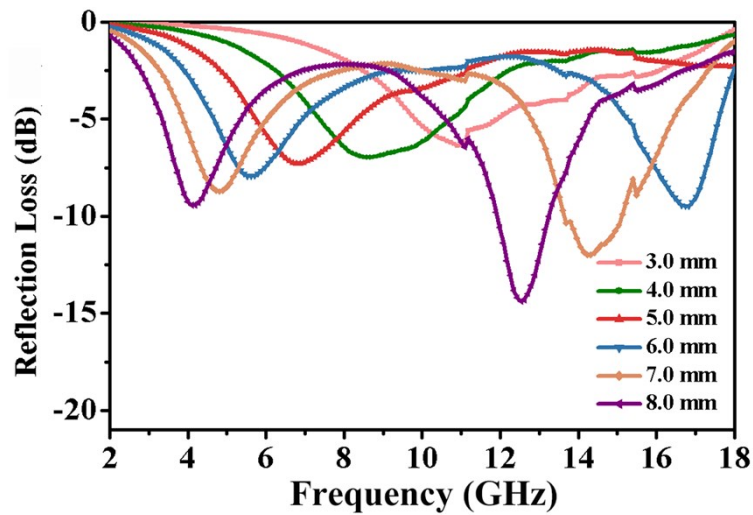


Fig. S7 The RL plots under specified thicknesses of MnO@C in 2-18 GHz.

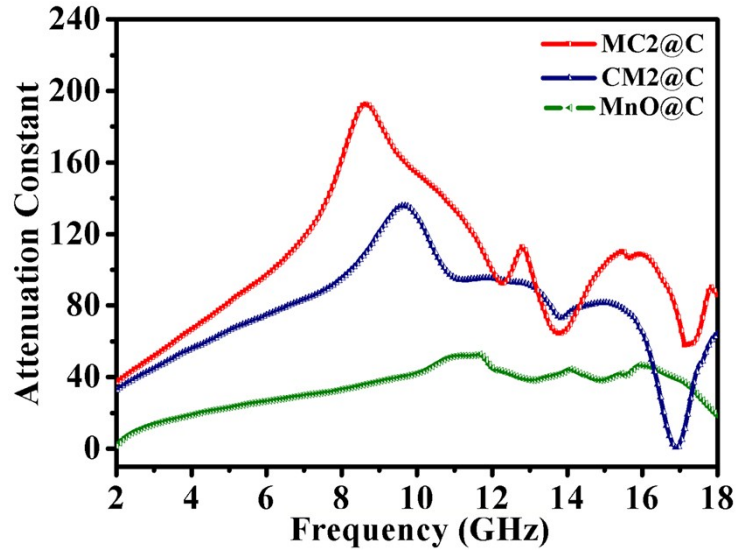


Fig. S8 Attenuation coefficients (α) of MnO@C, CM2@C and MC2@C against frequency.

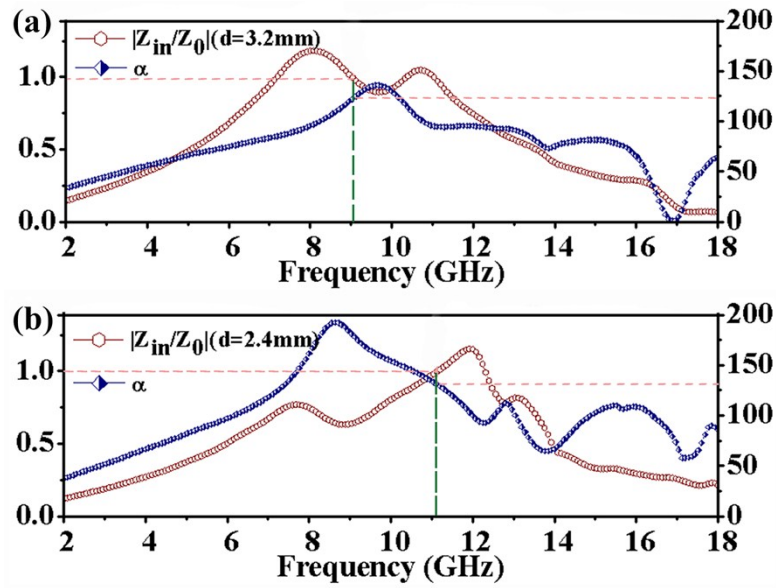


Fig. S9 Impedance matching ($|Z_{in}/Z_0|$) curves under the optimal thicknesses and attenuation coefficients (α) of CM2@C (a) and MC2@C (b).

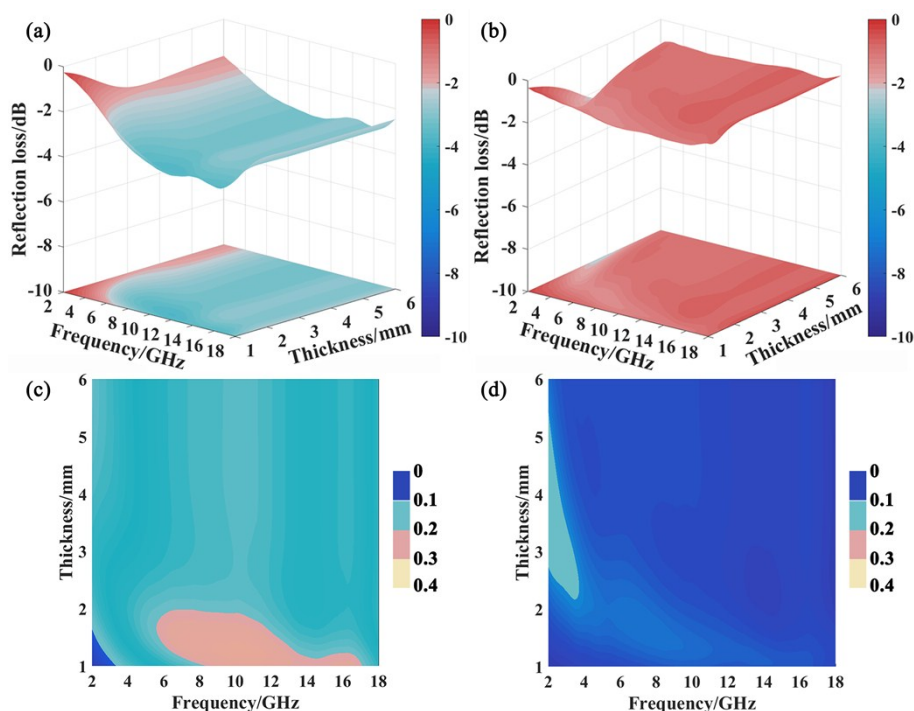


Fig. S10 Three-dimensional RL maps and the corresponding impedance matching maps of Co@C (a, c) and Co (b, d) specimens in 2-18 GHz.

The relative complex permittivity ($\epsilon_r = \epsilon' - j\epsilon''$) and the relative complex permeability ($\mu_r = \mu' - j\mu''$) of Co@C and Co specimens with the same mass loading were displayed in **Fig. S6**. Apparently, these two samples show much larger ϵ'' and μ'' values than Co/MnO@C composites, which represents the higher attenuation capability. However, the three-dimensional RL maps (**Fig. S10**) indicate that the EMW absorption performance of these two specimens is poor. The impedance matching maps of Co@C and Co specimens give the clue of poor performance. As shown in **Fig. S10**, the Z values (impedance matching values) of Co@C and Co specimens are located in the range of 0~0.3 and 0~0.2, respectively, which are far from the ideal impedance matching value ($Z=1$). This impedance mismatch results from the excessively high permittivity due to the large conductivity of Co.

References

- 1 Y. Jin, L. Wang, Q. Jiang, X. Du, C. Ji and X. He, *Materials Letters*, 2016, **177**, 85-88.
- 2 S. Guo, G. Lu, S. Qiu, J. Liu, X. Wang, C. He, H. Wei, X. Yan and Z. Guo, *Nano Energy*, 2014, **9**, 41-49.